

Article

Research on Wide Input Voltage LLC Resonant Converter and Compound Control Strategy

Kai Zhou ¹, Yang Liu ^{1,*} and Xiaogang Wu ^{1,2}

¹ Engineering Research Center of Automotive Electronics Drive Control and System Integration, Ministry of Education, Harbin University of Science and Technology, Harbin 150080, China

² State Key Laboratory of Automotive Safety and Energy, Tsinghua University, Beijing 100084, China

* Correspondence: liuyang736921@163.com; Tel.: +86-188-4597-2420

Abstract: This paper presents a wide input voltage vehicle DC/DC converter based on an LLC resonant converter for a 48 V light hybrid power system. According to the design requirements of on-board DC/DC converters and an analysis of their system characteristics, a full-bridge LLC resonant converter is employed with a zero-voltage activation of the switching transistors through resonant elements. In terms of the control strategy, the unsatisfactory high-frequency regulation gain of an LLC resonant converter is analyzed under the frequency modulation (FM) control strategy. In addition, to accommodate wide input voltage operating conditions, a composite control strategy is proposed by combining the advantages of the frequency modulation control strategy and phase shift control strategy, analyzing their control principles, and discussing the selection of the control mode switching point. By modeling LLC resonant converters with simulation software, the obtained results verify the effectiveness of the composite control strategy for LLC resonant converters. An experimental platform based on the TMS320F28335 controller, which can achieve stable operation with an input voltage in the range of 300 V–600 V and an output voltage of 48 V, is then built. The experimental results verify the feasibility of the design.

Keywords: LLC resonant converters; on-board DC/DC converters; wide input voltage; compound control



Citation: Zhou, K.; Liu, Y.; Wu, X. Research on Wide Input Voltage LLC Resonant Converter and Compound Control Strategy. *Electronics* **2022**, *11*, 3379. <https://doi.org/10.3390/electronics11203379>

Academic Editor: Raffaele Giordano

Received: 19 September 2022

Accepted: 17 October 2022

Published: 19 October 2022

Publisher's Note: MDPI stays neutral with regard to jurisdictional claims in published maps and institutional affiliations.



Copyright: © 2022 by the authors. Licensee MDPI, Basel, Switzerland. This article is an open access article distributed under the terms and conditions of the Creative Commons Attribution (CC BY) license (<https://creativecommons.org/licenses/by/4.0/>).

1. Introduction

With the shortage of energy supply and the degree of environmental pollution becoming more prominent, the development of vehicles powered by novel energy sources is becoming an important way to save energy and reduce pollution [1,2]. Notably, 48 V light hybrid vehicles serve as a transition from traditional fuel vehicles to pure electric vehicles. Compared to traditional systems, the 48 V hybrid systems add equipment such as motors and batteries. In addition to their auto start/stop function, they provide auxiliary power to the vehicle when necessary, and thus the 48 V system has the function of braking energy recovery to reduce emissions and fuel consumption. It can achieve more effective energy saving and emissions reduction and has good market application prospects [3,4].

In the 48 V hybrid system, the on-board DC/DC converter is the energy conversion unit between the high-voltage power battery and the low-voltage battery. It has one end connected to the power battery and the other end connected to the low voltage battery. It converts the high voltage of the power battery into low voltage to charge the low voltage battery, and it supplies power to the entire vehicle's low-voltage electrical equipment. A schematic diagram of the on-board DC/DC converter energy conversion scheme is shown in Figure 1.

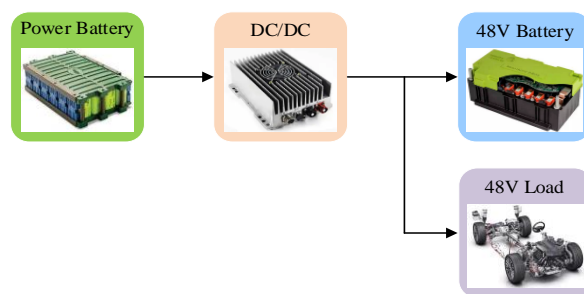


Figure 1. Energy conversion diagram for on-board DC/DC converters.

On-board DC/DC converters often use resonant converters to achieve electrical isolation of the input and output. The LLC resonant converters have a high performance, and the zero-voltage activation of their primary-side switching transistors is possible. In addition, the secondary rectifier can achieve zero-current shutdown. With these advantages, the LLC resonant converters are used in various applications with wide input voltages. New energy and communication power supply fields are rapidly developing. Therefore, the LLC resonant converters should also be adapted to wide input voltages. There are currently two main options for their implementation: an improved circuit topology and an improved control strategy.

To allow an LLC resonant converter to operate over a wider input voltage range, many researchers have conducted studies on the innovation of LLC resonant converters' topology. The authors of [5] propose an interleaved parallel LLC resonant converter, where a parallel connection is applied for the primary side circuit of the transformer of the two LLC resonant converters, while the secondary side of the transformer is a hybrid rectifier. The circuit structure is more complex, and it has a small operating frequency range. A converter with a three-bridge arm is presented in [6]. It is a hybrid combination of two full bridges where two auxiliary switches are added on the secondary side; thus, the zero-voltage activation and zero-current deactivation of all the switches can be achieved to maintain high efficiency over a wide range. The study in [7] proposes an LLC resonant converter with an auxiliary bidirectional switching unit. It can fully use the additional bidirectional switching unit when the input bus voltage decreases. This allows the converter to achieve high voltage gain and efficient normal operations with a large excitation inductance. The study in [8] proposes a dual-mode low-voltage DC converter. The entire input range is divided into two sections: a low input voltage range and a high input voltage range. The converters have two operating modes corresponding to these input voltage ranges. In the low input voltage range, the converter operates as a triple-switched double-ended actively clamped forward converter, while operating as an asymmetric half-bridge converter in the high input voltage range. The authors of [9] propose an LLC resonant converter capable of switching between full-bridge and three-level. The full bridge LLC resonant converter operates in the low input voltage range, while the three-level LLC resonant converter operates in the range of a high input voltage. However, the number of switches is high, and the circuit structure is complex, which is not conducive to parameter design. A modified two-transformer LLC resonant converter is proposed in [10]. In the latter, the gain is changed according to the change in the circuit structure and whether another transformer participates in the resonance. This topology adds many auxiliary devices, and the control strategy cannot achieve smooth switching between modes. An LLCC converter is proposed in [11]. In the latter, based on the traditional full bridge LLC resonant converter structure, an auxiliary capacitor is added in parallel with the resonant inductance. Under normal working conditions, the converter operates in LLC mode. When the input voltage increases, the auxiliary capacitor participates in the system's resonance, which increases the converter's gain range. Under this control mode, the current has high-order harmonics, which easily increases the circulating current of the system and reduces the overall efficiency.

Many researchers have determined the operating requirements of a wide range of input voltages by changing the control strategy. Typically, LLC resonant converters use a variable frequency (VF) control to regulate the output voltage. In VF control, the switching frequency is changed to obtain the desired voltage gain. Therefore, the switching frequency range is narrow in applications with a low input voltage range. However, a wide input voltage range requires a wide switching frequency variation range, which causes certain issues. Conventional LLC resonant converters have a wide range of switching frequency variation in order to obtain a wide voltage gain, which is not conducive to the design and optimization of magnetic components. When the input voltage is high, the converter needs a lower voltage gain to stabilize the output voltage; at this time, the switching frequency is high, resulting in increased converter losses and lower overall efficiency. There is a problem involving the unsatisfactory high frequency regulation gain of LLC resonant converters under a frequency control strategy [12–14]. In view of this situation, some researchers have proposed different control methods. For instance, a control strategy for adaptive phase shift regulation is proposed in [15]. This topology connects two half-bridges in series on the primary side. The rectifier filter side uses a power-switching transistor rather than a diode rectifier. Since the primary side is a double half-bridge series connection, the voltage stress on the switching transistors is greatly reduced. The input voltage range can be widened by adjusting the phase shift angle of the secondary switching transistor. The study in [16] proposes a T-type, three-level LLC resonant converter with an ultra-wide input voltage range. It uses a composite control strategy that integrates variable frequency control, phase shift control, and variable mode control. Compared with the conventional LLC resonant converter, this composite control strategy allows the gain ratio of the LLC resonant converter to be eight times higher. In [17], a novel control scheme is proposed for a stacked structure LLC resonant converter. During its normal operation, the frequency doubler modulation strategy is adopted to reduce the switching loss and driving loss, and the output is regulated by pulse frequency modulation (PFM). During the hold-up time operation, the pulse width modulation is adopted to increase the system voltage gain, and the switching frequency is fixed during this operation stage. With a different input voltage range, a hybrid control strategy is proposed to realize zero-voltage switching (ZVS) operation for all the switches of the proposed converter within a full power range in [18]. When at a high input voltage, extended phase shift control is applied to extend the ZVS range. When at a low input voltage, a variable gain LLC converter is designed to regulate the voltage distribution among the dual active bridge (DAB) converter and LLC converter for the ZVS operation of the DAB converter. A dual half-bridge, three-level LLC resonant converter is proposed in [19]. A wide-range control strategy is proposed for this topology to achieve gain adjustment by frequency modulation and pulse width modulation. The authors of [20] propose an integrated Buck-Boost LLC converter which is suitable for a wide input voltage range, while the common use of switch transistors reduces the number of used switches. With pulse width modulation and phase shift control, each switch on the primary side can perform zero-voltage activation in the full input voltage and load ranges. A dual-transformer-based LLC resonant converter is proposed in [21]. The output voltage is regulated through a fixed-frequency phase shift pulse width modulation control scheme. The proposed converter is capable of realizing soft switching over a wide input voltage and the entire load range. The study in [22] proposes a dual-bridge LLC resonant converter for wide input applications. The topology is an integration of a half-bridge LLC circuit and a full-bridge LLC circuit. The fixed-frequency pulse width-modulated control is employed and a range of twice the minimum input voltage can be covered.

This paper presents a wide input voltage vehicle DC/DC converter based on the LLC resonant converter for a 48 V light hybrid power system. Through the composite control modes of FM control and phase shift control, the problem of the unsatisfactory high frequency regulation gain of the LLC resonant converter under a frequency control strategy is solved. This is due to the fact that the phase shift control strategy is easier to implement than the frequency control strategy, and the fixed operating frequency is more favorable to

the optimization of the magnetic component's design. By combining the two methods via mixing the control, the circuit mode can be smoothly switched, and the output voltage can be stabilized, which enables the widening of the input voltage range, the performance of soft switching, and the improvement of work efficiency.

This paper is organized as follows. Section 2 introduces the LLC resonant converter's topology and characteristics' analysis. Section 3 discusses and analyzes the implementation of a composite control strategy by combining the advantages of frequency modulation and phase shift control methods. In Section 4, the design of essential parameters is detailed. The composite control model of the LLC resonant converter's topology is simulated and analyzed to verify the rationality of the composite control strategy in Section 5. In Section 6, an experimental platform with an input voltage of 300 V–600 V and an output voltage of 48 V is established to verify the feasibility of the design. Section 7 provides the conclusions.

2. LLC Resonant Converter Topology and Characteristics' Analysis

The topology of the LLC resonant converter is shown in Figure 2, which can be divided into an inverter network, a resonant network, and a rectifier filter network. The inverter network consists of switching transistors Q_1 – Q_4 . The resonant network consists of the resonant capacitor C_r , resonant inductance L_r , and excitation inductance L_m , while the resonant capacitor C_r also prevents the DC component of the square wave generator's output voltage flowing to the transformer while balancing the magnetic flux to prevent magnetic circuit saturation. The rectifier filter network is a double half-wave rectifier with a center tap on the secondary side of the transformer.

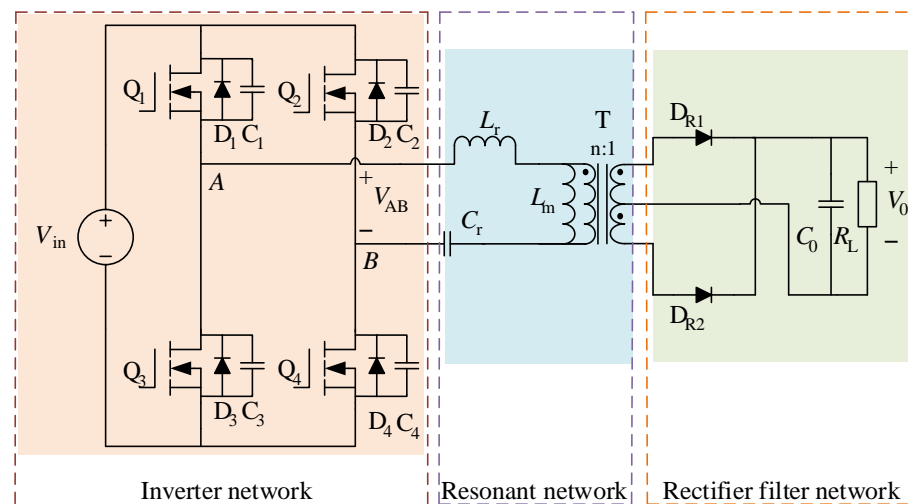


Figure 2. LLC resonant converter topology.

The LLC resonant converter has two resonant frequencies: the first resonant frequency, and the second resonant frequency:

$$f_r = \frac{1}{2\pi\sqrt{L_r C_r}} \quad (1)$$

$$f_m = \frac{1}{2\pi\sqrt{(L_r + L_m) C_r}} \quad (2)$$

If the driving signal frequency of the switching transistor is f_s , the analysis of the operating mode corresponds to when $f_m < f_s < f_r$; the operating waveform in this frequency range is shown in Figure 3. When the excitation current is equal to the resonant current, the voltage across L_m is no longer clamped, and L_r , C_r , and L_m resonate together. From Figure 3, it can be seen that the diode on the secondary side achieves zero-current shutdown.

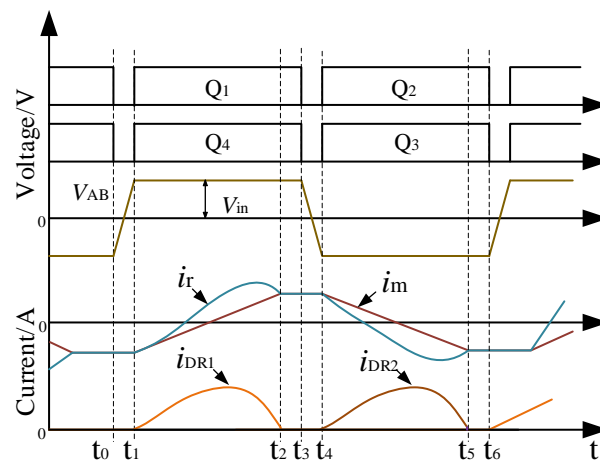


Figure 3. Main operating waveform when $f_m < f_s < f_r$.

The fundamental harmonic approximation method is used to establish the equivalent fundamental mathematical model of the LLC resonant converter [23]. The DC input voltage of the inverter network is V_{in} , as shown in Figure 2. The bridge arm’s diagonal switch transistor is simultaneously adjusted on and off, and the two groups of transistors perform complementary conduction; then, the resonant network input voltage V_{AB} has a duty cycle of 0.5. The amplitude of the periodic square wave is V_{in} . Figure 4 shows the equivalent topology diagram of the conversion of the rectifier filter network to the primary side of the transformer.

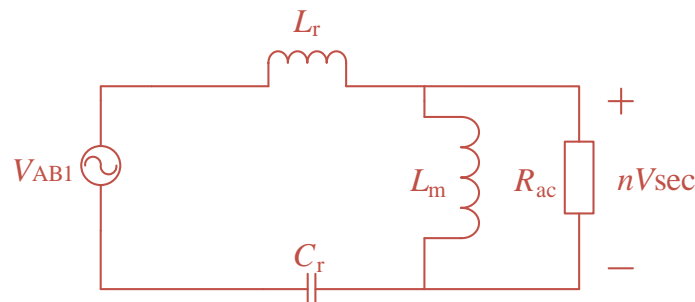


Figure 4. LLC resonant converter simplified circuit.

The equivalent resistance converted to the original side is given by:

$$R_{ac} = n^2 R_e = \frac{8n^2}{\pi^2} R_L \tag{3}$$

where n denotes the transformer’s primary to secondary turns.

The ratio of the transformer’s secondary voltage converted to the primary voltage is expressed as:

$$M = \frac{nV_o}{V_{in}} = \frac{nV_{sec}}{V_{AB1}} \tag{4}$$

where V_{AB1} is the input voltage of the resonant network after conversion; nV_{sec} is the output voltage of the resonant network after conversion.

The transfer function of a circuit $H(j\omega)$ is then simplified as:

$$H(j\omega) = \frac{nV_{sec1}}{V_{AB1}} = \frac{\frac{j\omega_s R_{ac} L_m}{R_{ac} + j\omega_s L_m}}{j\omega_s L_r + \frac{1}{j\omega_s C_r} + \frac{j\omega_s R_{ac} L_m}{R_{ac} + j\omega_s L_m}} \tag{5}$$

where ω_s is the switching angular frequency.

The ratio of the excitation inductance to resonant inductance is defined as:

$$\lambda = L_m/L_r \tag{6}$$

Afterwards, the quality factor is defined as:

$$Q = \frac{\sqrt{L_r/C_r}}{R_{ac}} \tag{7}$$

The voltage gain function can then be derived:

$$M(f_N) = |H(j\omega)| = \frac{1}{\sqrt{\left[\left(1 - \frac{1}{(f_N)^2}\right)Qf_N\right]^2 + \left[\left(1 - \frac{1}{(f_N)^2}\right)\frac{1}{\lambda} + 1\right]^2}} \tag{8}$$

where f_N is the normalized frequency, $f_N = f_s/f_r$.

Connecting all the peak gain curves in Figure 5 yields a purely resistive curve. If the above diagram is divided by a purely resistive curve and a straight line with $f_N = 1$, the converter can be divided into three operating zones:

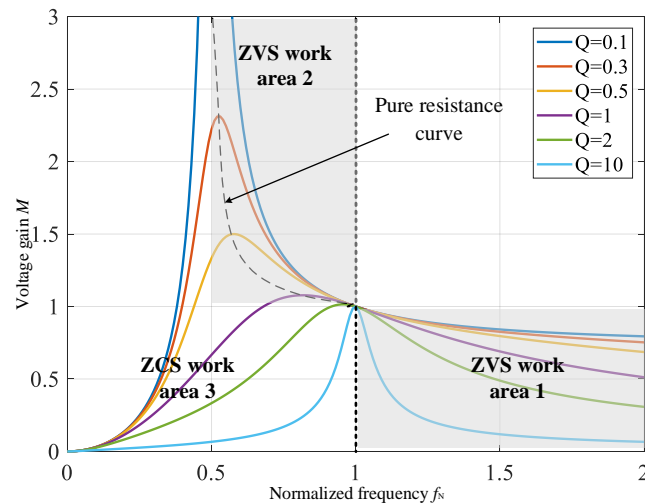


Figure 5. Voltage gain curve of a resonant network when the quality factor changes.

Region 1—the right side of the purely resistive curve and the right side of $f_N = 1$. At this time, the gain M is less than 1; in the inductive operating area, the buck mode is operational, and the LLC resonant converter is in the ZVS state.

Region 2—the right side of the purely resistive curve and the left side of $f_N = 1$. At this time, the gain M is more than 1; in the inductive operating area, the boost mode is operational, and the LLC resonant converter is in the ZVS state.

Region 3—the left side of the purely resistive curve and the left side of $f_N = 1$. At this time, the gain M is variable in the capacitance-operating area, and the LLC resonant converter is in the zero-current switching (ZCS) state.

In the design of a resonant topology, it is necessary to make it functional in the ZVS area, i.e., regions 1 and 2. While working in region 1, the rectifier transistor on the secondary side cannot achieve ZCS, which will reverse recovery, and the loss increases. Therefore, the LLC resonant converter performs best under FM control in region 2, which is the boost mode.

3. Composite Control Strategy

The characteristic analysis shows that the LLC resonant converter based on the FM control strategy can achieve soft switching in a certain gain range. However, with a wide

range of voltage inputs, the switching transistors require a large frequency regulation range, which is not conducive to the design optimization of the converter’s magnetic components. Consequently, another control method for LLC resonant converters, referred to as the phase shift control strategy, is introduced. The LLC resonant converters usually use two modulation methods (phase shift control and frequency control) to achieve circuit stability. Phase shift control is easy to implement but its input voltage range is narrow. Frequency control is highly effective, but the converter’s magnetic element design is difficult. In this paper, two control methods, phase shifting and frequency conversion, are combined and applied to an LLC resonant converter. Phase-shifting control operates at a high voltage input and the frequency conversion control at a low voltage input. This control method retains the advantages of phase shift control and accounts for the good characteristics of frequency control. This section discusses and analyzes the implementation of the composite control strategy by combining the advantages of the two control methods [24].

3.1. FM Control

Pulse frequency modulation is the most common control method for LLC resonant converters. The schematic diagram of the FM closed-loop control strategy of the LLC resonant converter is shown in Figure 6. The output voltage error of the resonant topology is derived by measuring the output voltage and then comparing it with the given reference voltage value. The driving signal of the switch is obtained through a proportional integral (PI) link in order to adjust the resonant topology’s output [25].

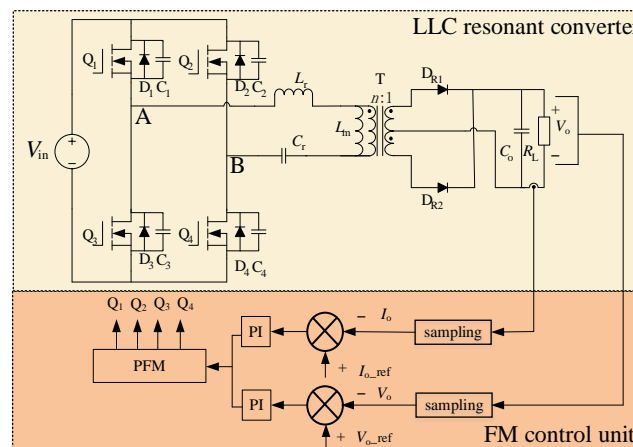


Figure 6. FM control strategy.

Resonant network voltage gain curve for different values of inductance ratio λ is shown in Figure 7. When the inductance ratio λ increases, the gain will decrease accordingly, and the input and output voltage range will become smaller. Therefore, the output signal is difficult to regulate in the case of a low input voltage. The frequency corresponding to the peak of the gain curve decreases as the inductance ratio λ increases. When f_r remains unchanged, the inductance ratio λ increases, and the switching frequency range becomes larger, which results in increasing the converter losses. Thus, it can be seen that the inductance coefficient of the converter should be as small as possible. In addition, when the resonant frequency is constant, the resonant inductance is also determined. Under this condition, if the inductance ratio decreases, the excitation inductance also decreases. Thus, the excitation current increases, and the loss increases. The resonant power supply efficiency will then be reduced; therefore, the inductance ratio λ should take a larger value. It can be deduced from this analysis that the inductance ratio should take the appropriate value. When the normalized frequency increases, the LLC resonant converter gain decreases. It can be seen that the circuit operates at low load and no load, and the switching frequency can be adjusted upwards. When operating at full load, the switching frequency can be adjusted downward to ensure a constant output voltage.

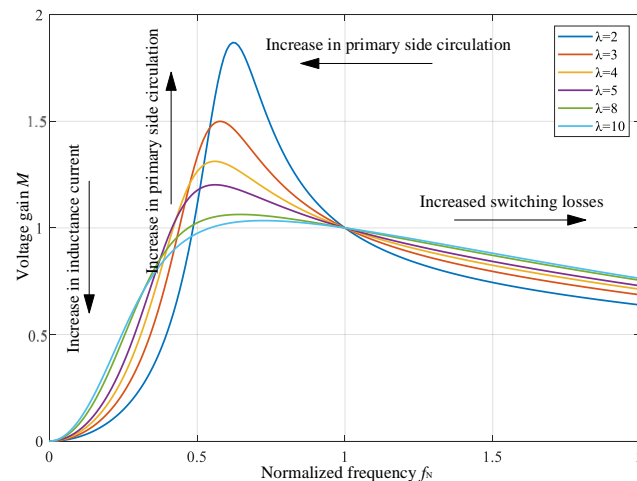


Figure 7. Resonant network voltage gain curve for different values of inductance ratio λ ($Q = 0.5$).

The LLC resonant converters operate at full, light, or no load. Too large of a range of frequencies will cause their losses to increase. It is also known from the gain formula that the input voltage is proportional to the normalized frequency. Therefore, the aim of the LLC resonant converter is to be suitable for a wide input voltage. Under the FM control strategy, the switching frequency range of the resonant converter should be increased. When the frequency is too high, the operating loss increases. While the frequency is too low, it is easy to be in the capacitance operating area and soft switching is unachievable. Therefore, too high and too low of a switching frequency under a wide input voltage makes the converter work inefficiently. The frequency adjustment range is limited to keep the output voltage constant.

In summary, in the case of uncertainty in Q and λ , the LLC resonant converter only works properly in a certain gain range. Based on the FM control mode, the only way to meet the wide input voltage operating conditions is by changing the upper and lower limits of the FM frequency. However, broadening the frequency causes many adverse effects that make it impossible for the converter to work efficiently. Therefore, to meet the wide input voltage operating conditions, the control strategy of the LLC resonant converter should be changed.

3.2. Phase Shift Control

The phase shift control method of the LLC resonant converter consists in fixing the operating frequency of the switching transistors so that it becomes equal to the resonant frequency, as well as changing the output characteristics of the resonant converter by adjusting the phase shift angle of the switching transistors of the inverter network. The phase shift angle of Q_1 – Q_4 is adjusted, which can be divided into two groups according to the phase angle difference between the leading bridge arm and the lagging bridge arm. Q_1 and Q_3 are leading bridge arms, while Q_2 and Q_4 are lagging bridge arms. The output characteristics are then changed by the phase angle difference between the leading and lagging bridge arm. The operating waveform in the phase shift mode is shown in Figure 8.

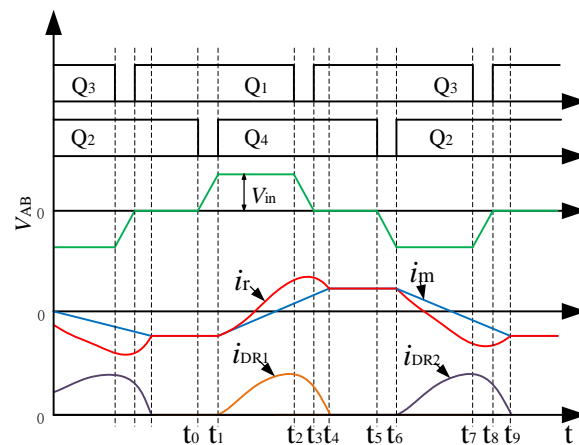


Figure 8. Phase shift control mode’s operating waveform.

The basic characteristics of the LLC resonant converters are assessed using time domain analysis [26,27]. The following system of equations can be derived based on the time domain analysis:

$$\begin{cases} -(1 + \cos \theta_2) \cdot I_m^* - \sin \theta_2 \cdot V_{Cr}^*(0) - M \cdot \sin \theta_2 + (\sin \theta_2 - \sin(\theta_2 - \theta_1)) = 0 \\ -(\theta_2 - \theta_3 + \sin \theta_2) \cdot I_m^* + (1 + \cos \theta_2) \cdot V_{Cr}^*(0) + (\cos \theta_2 - 1)M \\ \quad + (\cos(\theta_2 - \theta_1) - \cos \theta_2) = 0 \\ -\sin \theta_2 \cdot I_m^* + (\cos \theta_2 - 1) \cdot V_{Cr}^*(0) + \left(\cos \theta_2 - 1 - \frac{8\theta_3}{\pi^2} Q\right) M \\ \quad + (\cos(\theta_2 - \theta_1) - \cos \theta_2) = 0 \end{cases} \quad (9)$$

where θ_1, θ_2 , and θ_3 are the angles at moments t_2, t_4 , and t_5 , respectively; I_m^* is the current standard value when the excitation current and resonance current are equal; and $V_{Cr}^*(0)$ is the resonant capacitor’s zero-moment voltage standard value.

θ_1, θ_3 , and I_m^* are expressed as:

$$\theta_1 = \pi D_y / f_N \quad (10)$$

$$\theta_3 = \pi / f_N \quad (11)$$

$$I_m^* = M\theta_2 / (2\lambda) \quad (12)$$

where D_y is the duty cycle.

In the reference variable, λ and f_N can be identified as known quantities. In addition, the load condition determines the quality factor Q . Figure 9 shows the variation curve of the duty cycle D_y versus the input–output voltage ratio M for different values of the quality factor Q . In the graph, the inductance factor is taken as 4, and the normalized frequency is $f_N = 1$.

It can be seen from Figure 9 that in the phase shift control mode, the normalized frequency is kept at 1, and the voltage at the load side changes by adjusting the duty cycle. When the duty cycle is 1, the input to output voltage ratio is 1. The output voltage is maximum at this time, while for the rest of the time, as the duty cycle D_y changes, the value of M is less than 1. Under the phase shift mode control, the LLC resonant converter operates in step-down mode. It can also be clearly seen from Figure 5 that the gain characteristics of the resonant converter are difficult to adjust in terms of frequency when operating in region 1. Based on the FM control strategy, the rectifier on the secondary side of the transformer cannot achieve ZCS. Therefore, there is a reverse recovery problem and the loss increases. Thus, the phase shift control strategy makes up for the shortcomings of the FM control strategy in the buck mode. The phase shift control strategy is shown in Figure 10.

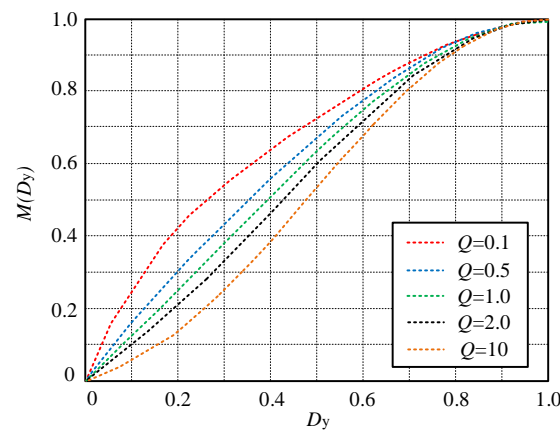


Figure 9. Input to output voltage ratio in phase shift control mode.

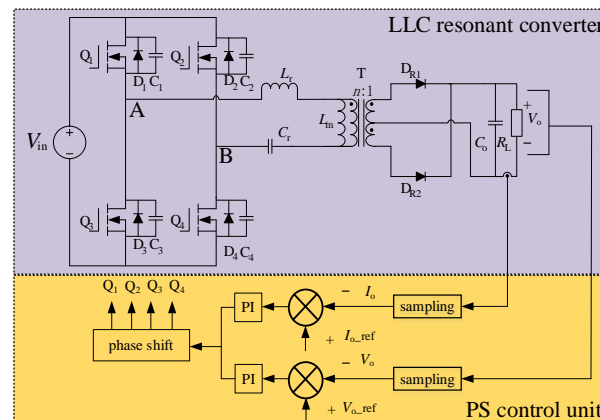


Figure 10. Phase shift control strategy.

3.3. Composite Control

The LLC resonant converter cannot achieve a wide gain range under a single control method. Under frequency control, the gain can only be greater than 1 in order to ensure the soft switching of both the primary and secondary sides, and the maximum voltage gain of the frequency control will be limited due to the influence of the quality factor of the system. Under the phase shift control within the primary side, the gain can only be less than 1. Therefore, the following composite control strategy is proposed.

When $M > 1$ (the resonant network boost conversion), the FM control strategy is used, and the resonant network gain decreases as the regulated switching frequency increases, which applies to the case of a low input voltage.

When $M = 1$ (the resonant network equals voltage conversion), only L_r and C_r co-resonance takes place. f_r is taken as the highest switching frequency. This is the mode-switching point of the two control strategies. That is, when $f_s = f_r$, the phase shift angle is 0, the electrical energy is directly converted, and the converter efficiency is at its best.

When $M < 1$ (the resonant network buck conversion), the phase shift control strategy is used. $f_s = f_r$ is retained. As the regulation duty cycle decreases, the resonant network gain decreases, which is suitable for the case of a higher input voltage.

Too low or too high of an input voltage will cause the system loss to increase, thus affecting the efficiency of the LLC resonant converter. Therefore, to maintain the efficiency of the LLC resonant converter, it is important to design an appropriate input voltage range. In addition, the voltage at the switching point should be comprehensively considered to make the mode switching of the LLC resonant converter as smooth as possible, which is conducive to optimizing the efficiency of the LLC resonant converter.

Figure 11 shows the block diagram of the composite control system of the LLC resonant converter. The LLC resonant converter’s output voltage is V_0 , and the resonant frequency is set as the switching frequency by comparing it with the given reference voltage V_{0_ref} . When the operating frequency of the resonant converter is less than the set value, the phase shift angle is equal to 1, and the FM mode is used to change the frequency f_s of the switching transistor to adjust the output voltage V_0 . However, increasing the resonant converter’s operating frequency to the set value still cannot regulate the voltage. The operating frequency is maintained as the resonant frequency is unchanged, and the phase shift angle d_s is changed to adjust the output voltage V_0 . Depending on the input voltage, the control strategy switches the mode to change only one of the variables, the frequency or phase angle, ensuring independence between the two.

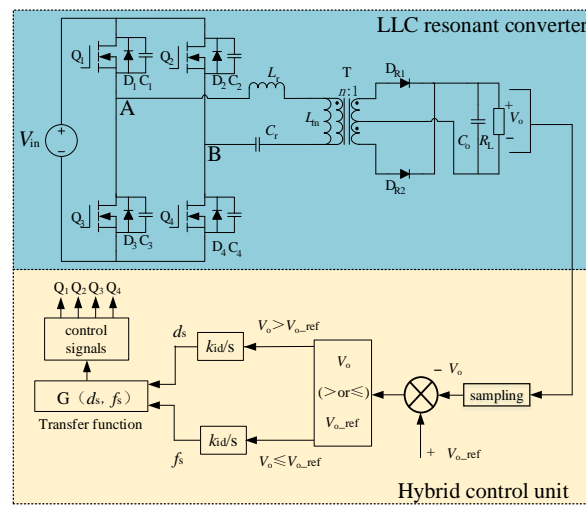


Figure 11. Block diagram of the composite control system.

It can be seen from Figure 5 that the converter should operate in region 2 for the best performance in the case of FM control, where the sub-side rectifier can realize ZCS, and, therefore, $f_s \leq f_r$ is selected. Since the efficiency is highest and the loss is lowest when $m \cdot \omega_s = \omega_r$ and the frequency remains the same in the case of phase-shifting control, the resonant frequency is chosen as the operating frequency in this case. Based on the above analysis, the mode-switching point selects the point where the operating frequency is the resonant frequency when the resonant network gain is 1, and the switching transistor duty cycle is 1.

Since the converter should be suitable for wide input voltages, in this paper, the minimum value of the input voltage, V_{in_min} , is set to one-half the maximum value of the input voltage, V_{in_max} :

$$V_{in_min} = \frac{1}{2} V_{in_max} \tag{13}$$

It is known from the basic principle of composite control that when the input voltage has its lowest value, the FM control mode holds and the resonant network gain attains the maximum value, $M(f_N)_{max}$. Correspondingly, when the input voltage is the highest value, the phase shift control mode holds, and the resonant network gain is the minimum value, $M(D_y)_{min}$. Since the output voltage is kept constant, then:

$$V_{in_min} \cdot M(f_N)_{max} = V_{in_max} \cdot M(D_y)_{min} = nV_0 \tag{14}$$

Since the boost is in the FM mode and the buck is in phase shift mode, by combining Equations (13) and (14), the following can be derived:

$$\begin{cases} 1 \leq M(f_N)_{\max} \leq 2 \\ 0.5 \leq M(D_y)_{\min} \leq 1 \end{cases} \quad (15)$$

By combining the working principle of the composite control strategy and the analysis of Figure 5, it can be deduced that the switching frequency should be greater than the frequency corresponding to the peak gain of the resonant network with a certain margin. To facilitate gain regulation, the switching frequency is set as the minimum operating frequency of the switching transistor [28].

In this paper, during the selection of inductance ratio, λ is set to 3. Figure 12 shows the frequency gain curve at this time.

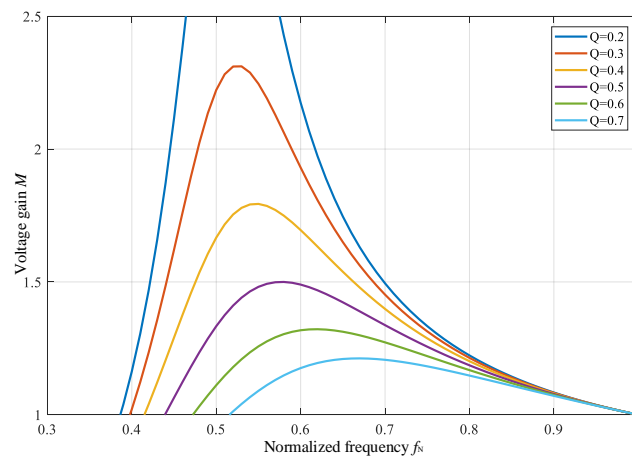


Figure 12. Frequency versus gain curve for $\lambda = 3$.

To improve the efficiency, a larger Q value is chosen within a reasonable range. According to the definition of the quality factor Q , when the LLC resonant converter operates at full load, the quality factor is taken as Q_{\max} . In addition, it can be seen in the frequency gain curve that the gain M decreases with the increase in Q . To ensure that the voltage increase in the rated operating condition is large enough, this paper considers that the gain of the lower limit of the input voltage V_{in_min} is $M(f_N)_{\max}$ in the rated operating condition. At this time, the quality factor Q takes the maximum value Q_{\max} , and $Q_{\max} = 0.5$ is considered. Figure 12 shows that in the leaving margin, $M(f_N)_{\max}$ and f_{N_min} are 1.33 and 0.75, respectively. It can be deduced from Equation (14) that the control mode's switching point voltage is:

$$V_{in_switch} = V_{in_min} \cdot M(f_N)_{\max} = 1.33V_{in_min} \quad (16)$$

The minimum gain $M(D_y)_{\min}$ can then be derived:

$$M(D_y)_{\min} = M(f_N)_{\max} / 2 = 0.67 \quad (17)$$

At this point, the corresponding minimum duty cycle is $D_{y_min} = 0.42$.

It can be easily surmised that the switching frequency is the minimum frequency f_{s_min} for different input voltages and loads, while the high-voltage, full-load duty cycle approximately reflects the minimum duty cycle, which is considered as the minimum duty cycle D_{y_min} .

4. System Parameter Design

The key technical parameters of the LLC resonant converter are shown in Table 1.

Table 1. Key technical parameters of the LLC resonant converter.

Symbol	Description	Value
V_{in_min}	Minimum input voltage	300 V
V_{in_max}	Maximum input voltage	600 V
V_o	Rated output voltage	48 V
f_r	Resonant frequency	100 kHz
f_{s_max}	Maximum switching frequency	100 kHz
f_{s_min}	Minimum switching frequency	75 kHz

From (16), the control mode switching point voltage can be obtained:

$$V_{in_switch} = 1.33V_{in_min} = 400 \text{ V} \quad (18)$$

It can be seen that when the input voltage is in the range of 300–400 V, FM control is used. When the input voltage is in the range of 400–600 V, phase shift control is used. Therefore, the transformer's turns ratio is calculated as:

$$n = \frac{V_{in_switch}}{V_o + V_F} = \frac{400}{48 + 0.966} \approx 8.2 \quad (19)$$

where V_F is the diode's on-state voltage drop, taking the value of 0.966 V.

In this paper, the inductance ratio is set to $\lambda = 3$, and the quality factor is $Q = 5$. This is the basis for the specific design of the resonant element parameters [29].

The load resistance of the LLC resonant converter at rated operating conditions is given by:

$$R_{Ld} = \frac{V_o^2}{P_o} = \frac{48^2}{2000} = 1.152 \text{ } \Omega \quad (20)$$

The equivalent resistance of the resonant network is expressed as:

$$R_{ac} = \frac{8n^2}{\pi^2} R_{Ld} = \frac{8 \times 8.2^2}{\pi^2} \times 1.152 = 62.8 \text{ } \Omega \quad (21)$$

The resonant frequency is $f_r = 100$ kHz, and the resonant capacitance is given by:

$$C_r = \frac{1}{\omega_r Q R_{ac}} = \frac{1}{2\pi f_r Q R_{ac}} = 50.7 \text{ nF} \quad (22)$$

The resonant inductance is computed as:

$$L_r = \frac{1}{\omega_r^2 C_r} = \frac{1}{(2\pi f_r)^2 C_r} = 49.97 \text{ } \mu\text{H} \quad (23)$$

The excitation inductance is given by:

$$L_m = \lambda L_r = 3 \times 49.97 = 149.91 \text{ } \mu\text{H} \quad (24)$$

5. Simulation Analysis

The composite control model of the LLC resonant topology is simulated and analyzed to verify the rationality of the composite control strategy. The simulation parameters are presented in Table 2. The simulation model is shown in Figure 13.

Table 2. Parameters of the simulated circuit.

Symbol	Description	Value
L_r	Resonant inductance	49.97 μH
C_r	Resonant capacitor	50.7 nF
L_m	Excitation inductance	149.91 μH
N	Transformer ratio	8.2
C_o	Filter Capacitor	2000 μF
V_{in}	DC input voltage	300–600 V
V_o	DC output voltage	48 V

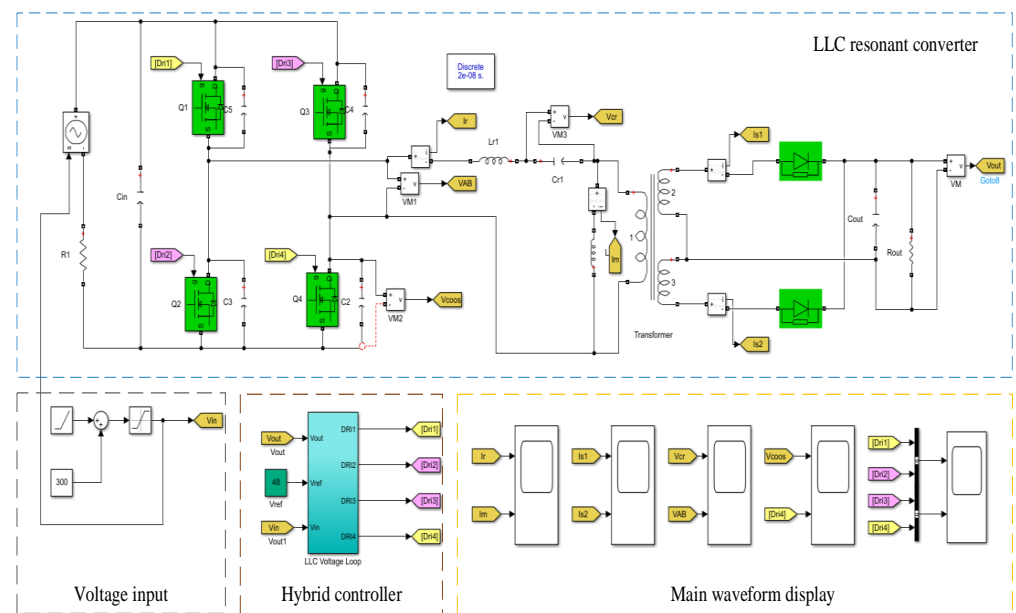


Figure 13. LLC resonant converter simulation model.

The simulation analysis is performed for the following three cases of input voltage to better verify the feasibility of the composite control strategy.

5.1. Output Voltage Waveform at Different Input Voltages

Figure 14 shows the input and output voltage waveforms when the input voltage is 300 V and then starts to linearly increase at 3 ms, reaching 600 V in 45 ms. It can be seen that when the input voltage linearly increases, the output voltage is maintained at 48 V, and when the boost voltage reaches the mode switching point voltage of 400 V, the output voltage can quickly return to constant after a small shake due to the control mode switching.

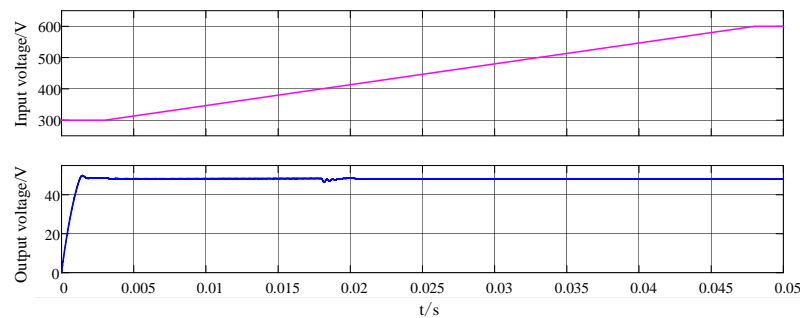


Figure 14. Input voltage from low to high, linearly increasing input and output voltage waveform.

Figure 15 shows the input and output voltage waveforms of the LLC resonant converter when the initial input voltage is 400 V and then changes abruptly to 600 V at 5 ms.

When the input voltage changes abruptly to 600 V, the LLC resonant converter switches to phase-shifting control, and small momentarily fluctuations are observed in the output voltage, which can then still maintain a constant value of 48 V.

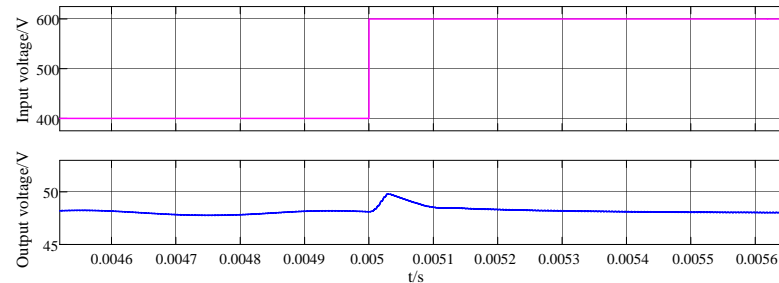


Figure 15. Input and output voltage waveform when the input voltage undergoes an abrupt change.

Figure 16 shows the LLC resonant converter’s input and output voltage waveforms when the initial input voltage is 400 V and then suddenly changes to 300 V at 5 ms. When the input voltage suddenly changes to 300 V, the LLC resonant converter switches to FM control. In the case of a sudden change in the input voltage, small transient fluctuations exist in the output voltage, which still can maintain a constant output of 48 V.

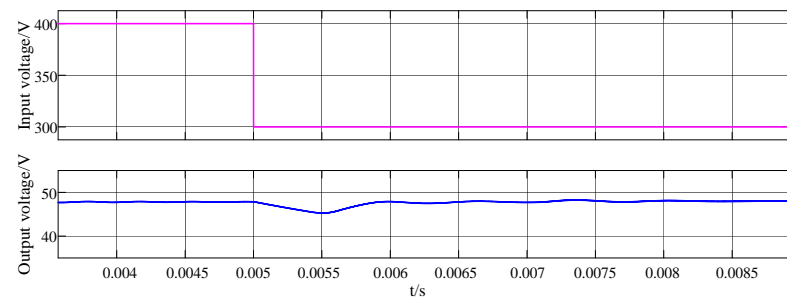


Figure 16. Input and output voltage waveform when the input voltage suddenly decreases.

5.2. Other Major Waveform

The FM mode waveforms of the resonant inductance and excitation inductance currents, i_r and i_m , are shown in Figure 17. The phase shift mode waveform is shown in Figure 18, and the overall waveform is shown in Figure 19.

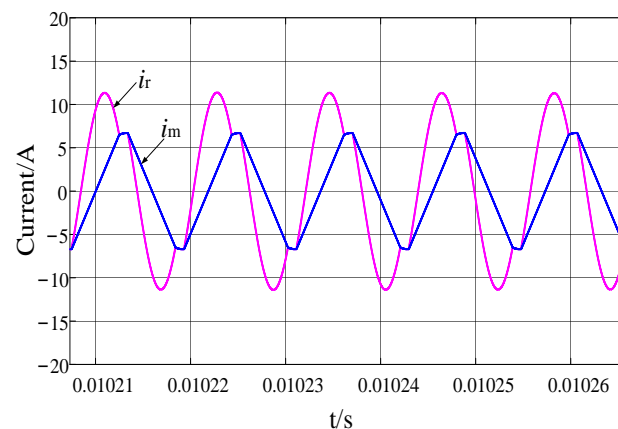


Figure 17. FM control mode waveform.

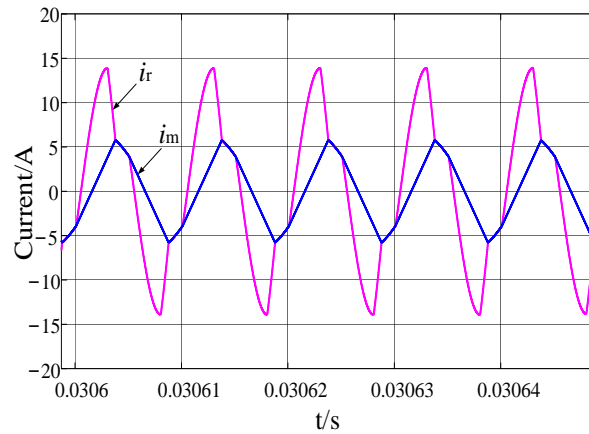


Figure 18. Phase shift control mode waveform.

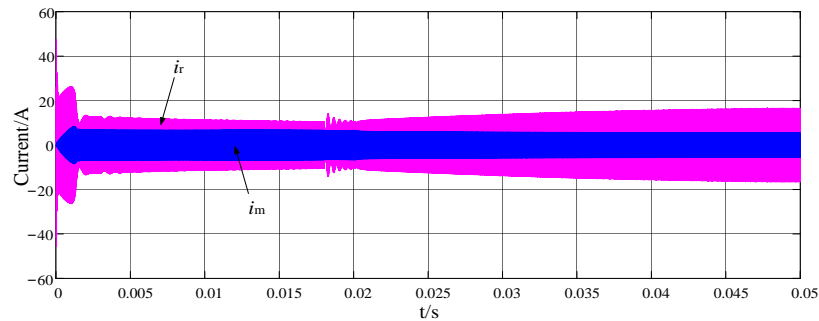


Figure 19. Overall waveform.

The rectifier diode’s current i_{s1} and i_{s2} waveforms are shown in Figures 20 and 21, respectively. It can be seen the LLC resonant converter can achieve the ZCS of the secondary side rectifier in both the FM and phase shift modes.

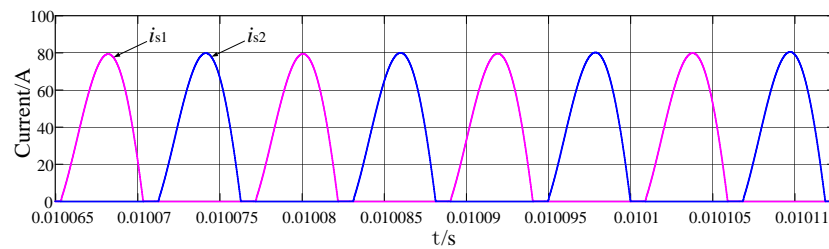


Figure 20. FM control mode waveform.

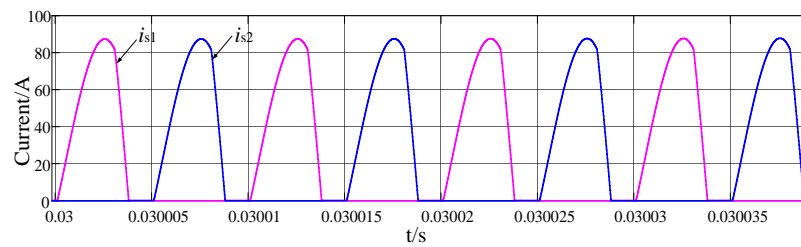


Figure 21. Phase shift control mode waveform.

The voltage, V_{Cr} , waveform at both ends of the resonant capacitor is shown in Figures 22 and 23. After regulating the control strategy, the resonant capacitor voltage is an AC waveform with an amplitude of 400 V.

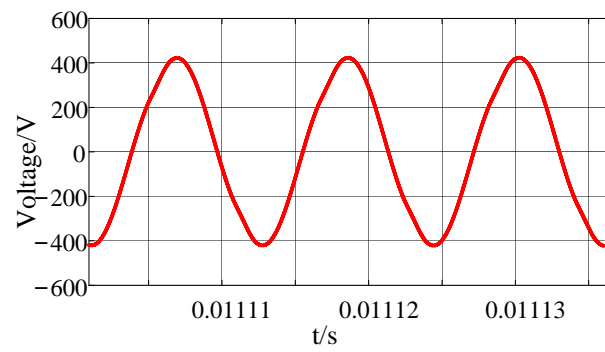


Figure 22. FM control mode waveform.

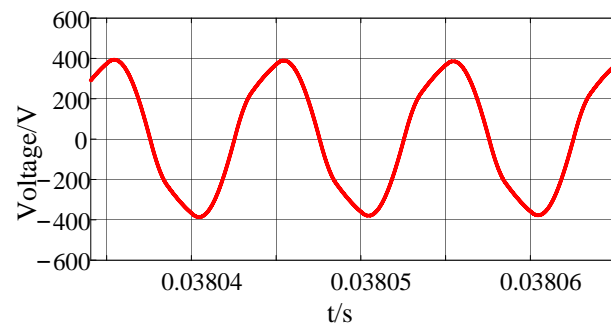


Figure 23. Phase shift control mode waveform.

The input voltage (V_{AB}) waveform of the resonant network is shown in Figures 24 and 25. The input voltage waveform of the resonant network for different DC voltage inputs is consistent with the principle analysis of the different control strategies that were presented in the previous section.

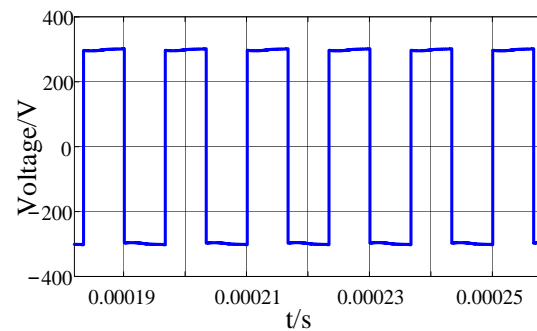


Figure 24. Waveform at 300 V DC input voltage.

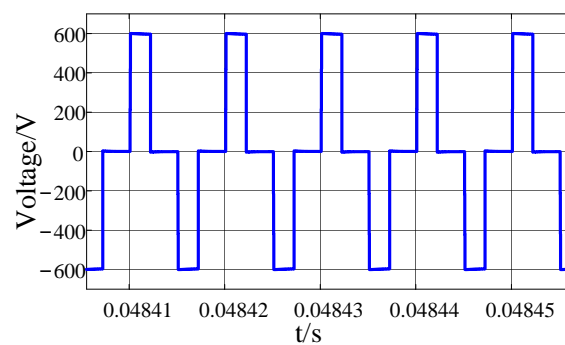


Figure 25. Waveform at 600 V DC input voltage.

The switching transistor drive waveforms are shown in Figures 26 and 27. In the FM mode, the Q_1 and Q_3 drive waveforms are complementary, and the Q_2 and Q_4 are synchronized with the Q_3 and Q_1 drive waveforms, respectively. In the phase shift mode, the Q_1 and Q_3 drive waveforms are ahead, while the Q_2 and Q_4 drive waveforms are lagging.

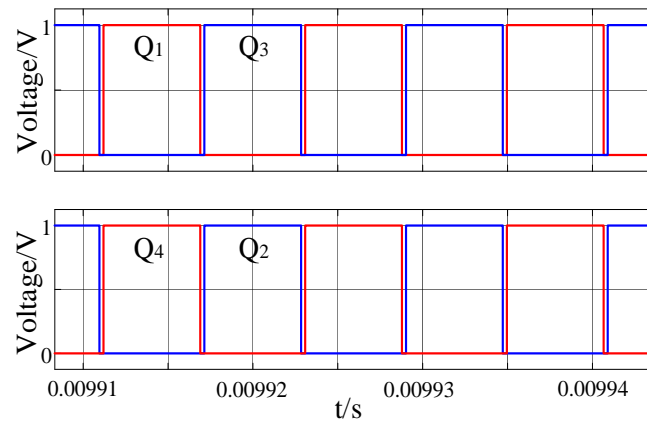


Figure 26. FM control mode.

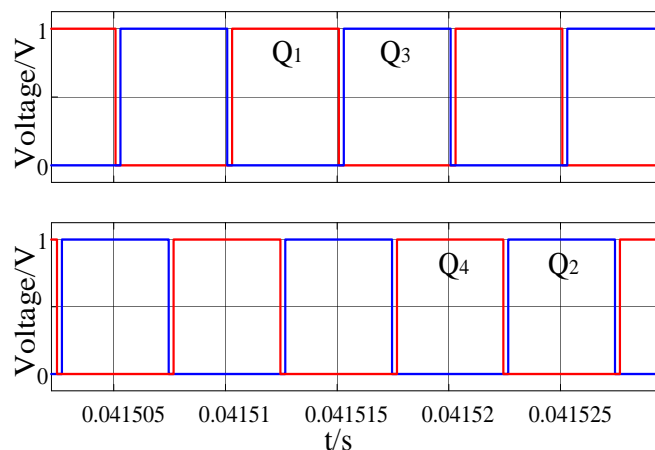


Figure 27. Phase shift control mode.

Therefore, it can be deduced from the above analysis that the LLC resonant converter can efficiently operate over the designed wide input voltage range and maintain a constant output.

6. Experimental Verification

Figure 28 shows the LLC resonant converter's software and hardware architecture. The TMS320F28335 digital signal processor is considered the LLC resonant converter's main control chip, and the experimental prototype of the LLC resonant converter is built based on the designed circuit parameters. The experimental main data are shown in Table 3. Figure 29 shows the experimental test platform.

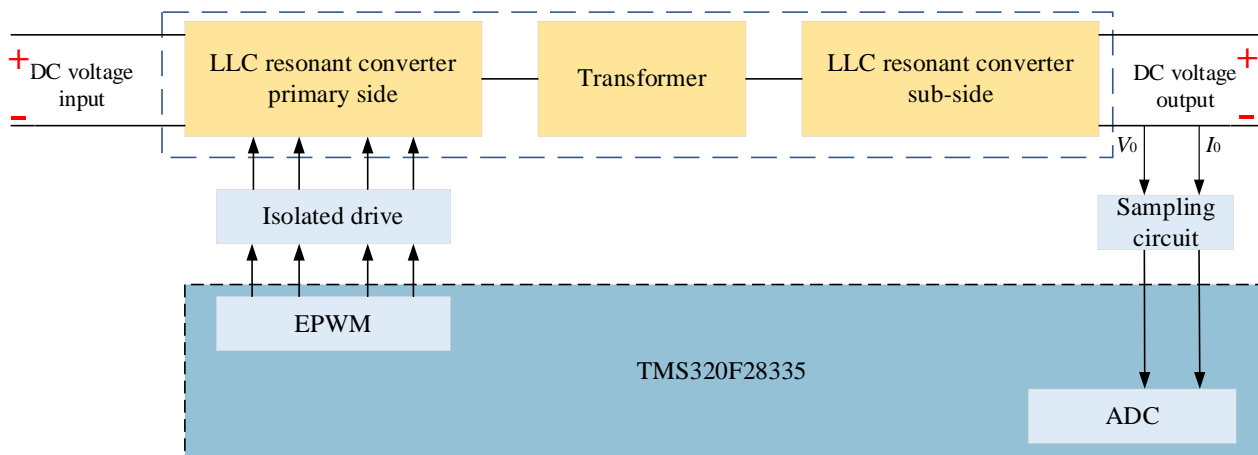


Figure 28. LLC resonant converter software and hardware architecture.

Table 3. Experimental main data.

Symbol	Description	Value
L_r	Resonant inductance	50 μ H
C_r	Resonant capacitor	51 nF
L_m	Excitation inductance	150 μ H
N	Transformer ratio	8.2
C_o	Filter Capacitor	2000 μ F
V_{in}	DC input voltage	300–600 V
V_o	DC output voltage	48 V

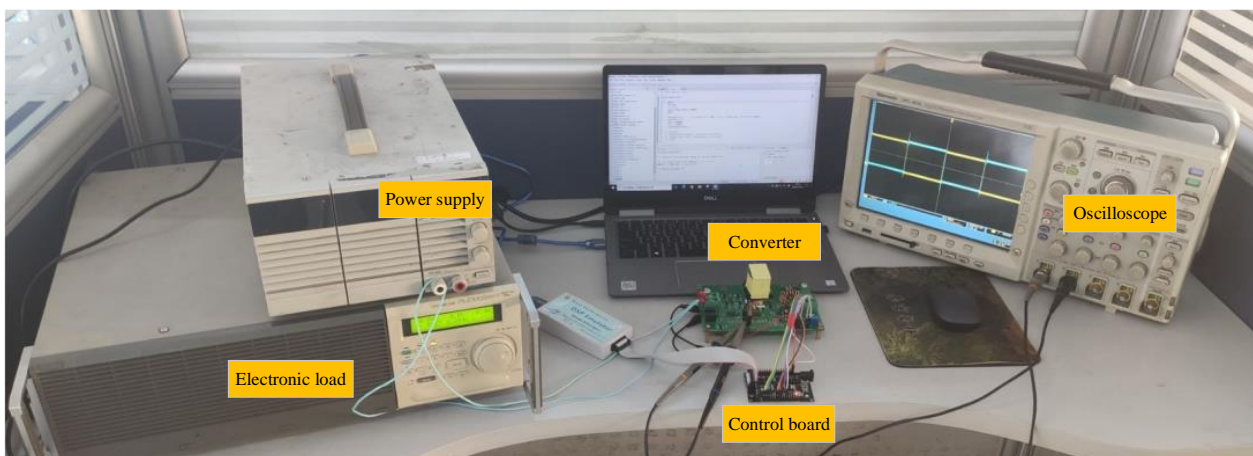


Figure 29. Experimental test platform.

Figure 30 shows the waveforms of the drive signal of the switch transistor Q_1 in FM mode and Phase shift mode. It can be seen that the voltages at the two ends of the switch transistor and the drive signal exhibit slight interleaving. That is, the voltage at the end of the switch transistor has dropped to 0 before the drive signal drives on it, and, thus, the ZVS is achieved. Due to the stray capacitance, the voltage hysteresis across the switching transistor increases and the deactivation loss is reduced. The rest of the switching transistors are similar to Q_1 .

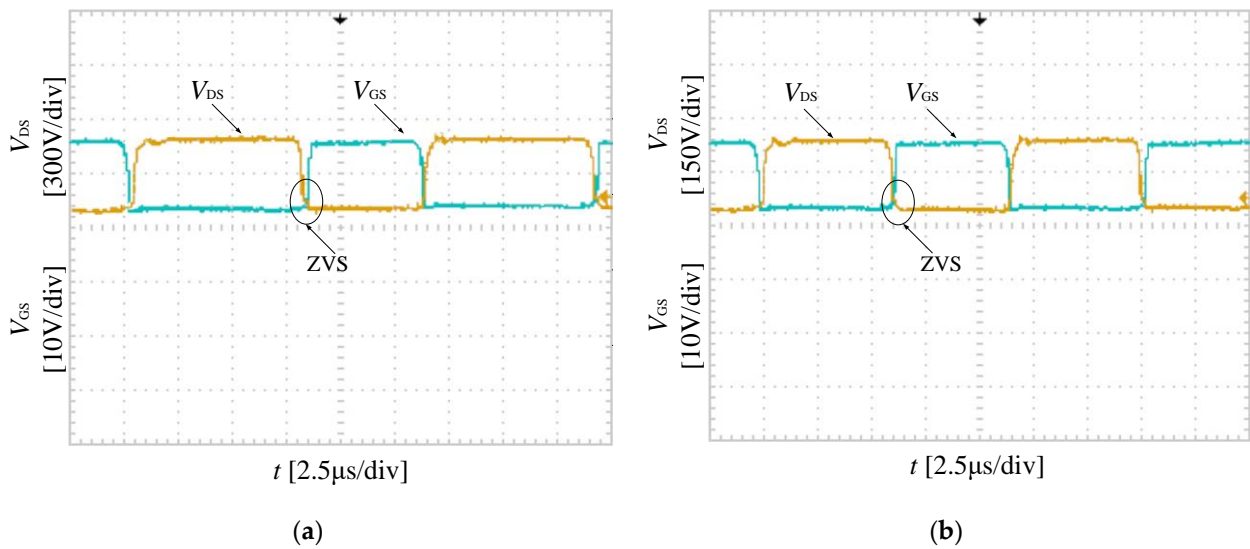


Figure 30. Switching transistor Q_1 drive signal. (a) FM mode switching transistor drive signal; (b) Phase shift mode switching transistor drive signal.

To demonstrate the applicability of the composite control strategy of the LLC resonant converter over a wide voltage range, the input voltage is boosted from 300 V to 600 V. The experimental waveform is shown in Figure 31a. At this time, the control switch transistor first undergoes a frequency modulation and then a phase shift. The voltage across the resonant capacitor and inductance current tends to smooth with the test time. The output voltage is almost constant at 48 V. The input voltage is then reduced from 600 V to 300 V, and the actual value is lower than 300 V, and then it finally increases. The experimental waveform is shown in Figure 31b. At this time, the chip controls the switching transistor’s first phase shift and then the frequency regulation. The voltage across the resonant capacitor and inductance current first increases and then decreases, while the output voltage is reduced to almost 25 V, followed by the input voltage’s increase to 85 ms to maintain a constant value of 48 V.

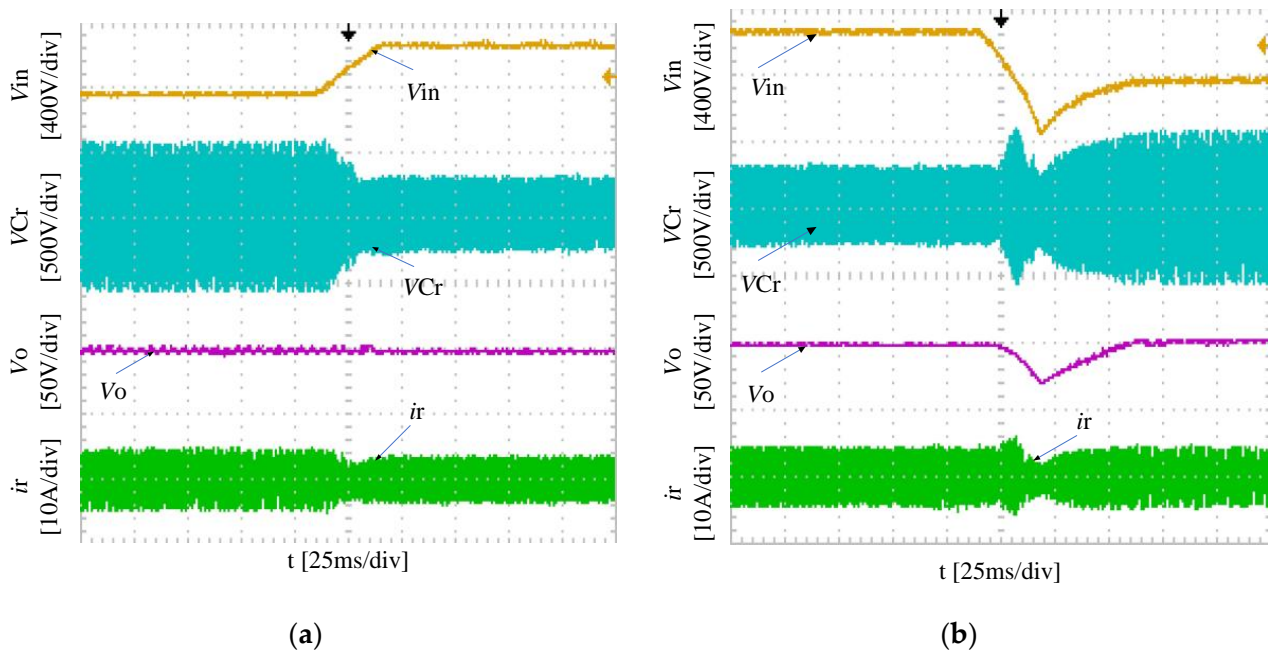


Figure 31. Voltage surge experimental waveform. (a) 300 V increased to 600 V; (b) 600 V reduced to 300 V.

Figures 32–34 show the experimental waveforms at a light load (10% full load), half load, and full load in FM mode (300 V input) and phase shift mode (500 V input), respectively. The waveforms of V_{AB} , V_{Cr} , and i_r in the resonant network are shown. Figure 34a shows the waveform of V_{AB} , V_{Cr} , and i_r in the resonant network when the input voltage is 300 V at full load. At this time, the switching frequency is 75 kHz. Figure 34b shows the waveform of V_{AB} , V_{Cr} , and i_r in the resonant network when the input voltage is 500 V at full load. At this time, the switching frequency is 100 kHz. In the FM control mode, V_{AB} is approximated as a square wave with an amplitude of 300 V, and V_{Cr} is approximated as an AC waveform of 300 V. In the phase shift control mode, V_{AB} shows a stepped waveform and V_{Cr} is an AC waveform of approximately 500 V. The voltage and current waveforms of the resonant network for different DC voltage inputs are consistent with the previous analysis. Figure 35 shows the waveform at no load and with full load switching applied. The output voltage exhibits a small fluctuation when the load is switched, and finally the output voltage is stabilized at 48 V. The experimental results and theoretical analysis show that in the full voltage and full load range, the converter can operate well in FM mode and phase shift mode.

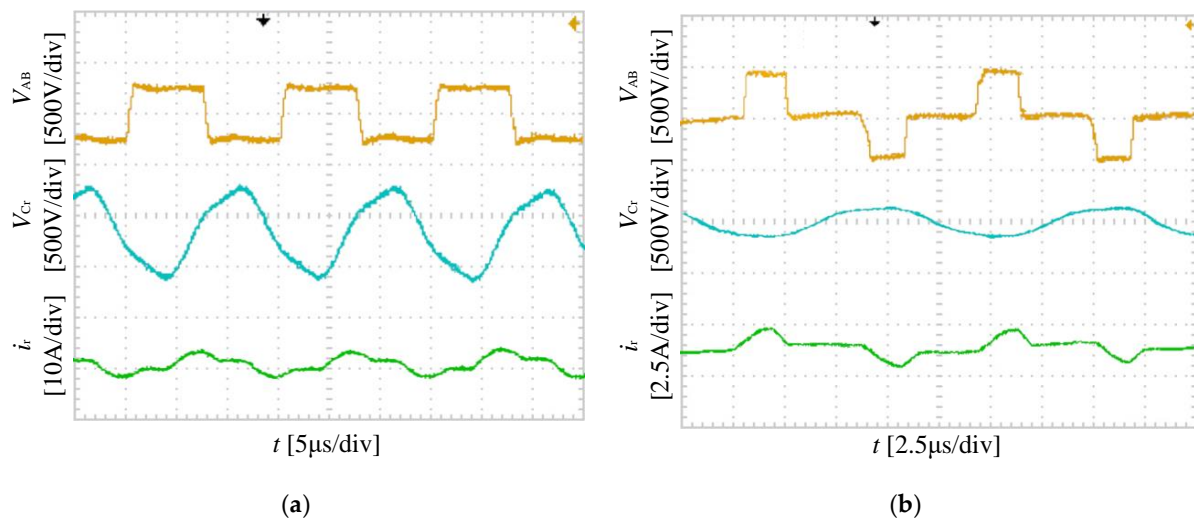


Figure 32. Light load (10% full load) experimental waveform. (a) 300 V input (FM mode); (b) 500 V input (Phase shift mode).

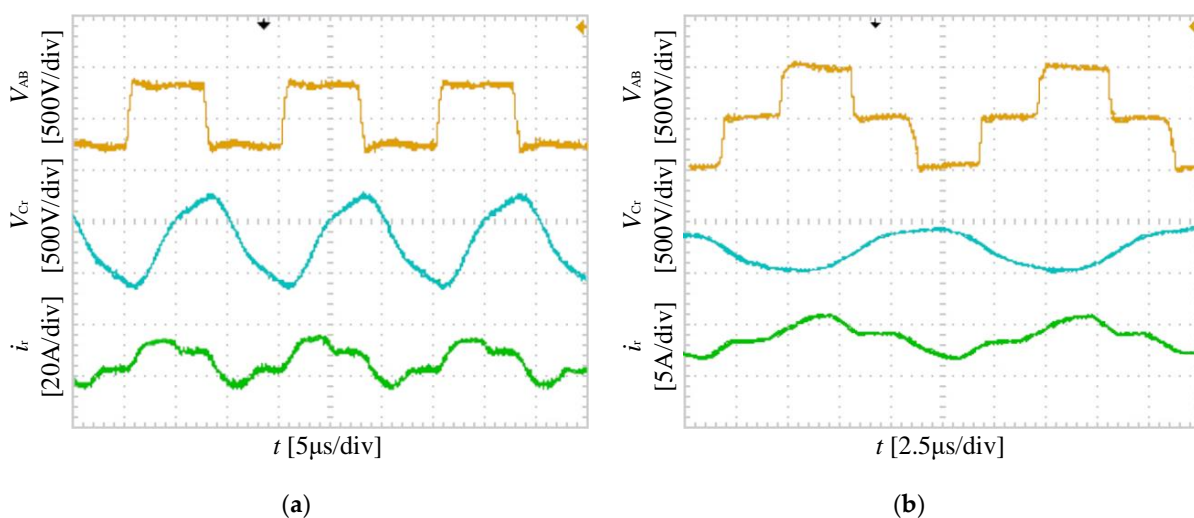


Figure 33. Half load experimental waveform. (a) 300 V input (FM mode); (b) 500 V input (Phase shift mode).

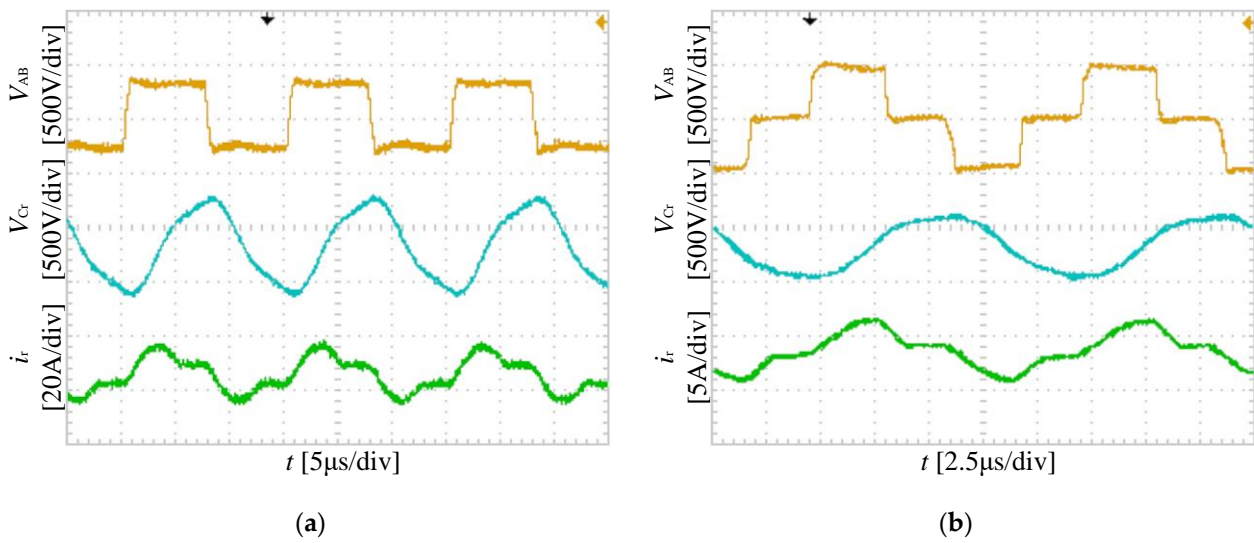


Figure 34. Full load experimental waveform. (a) 300 V input (FM mode); (b) 500 V input (Phase shift mode).

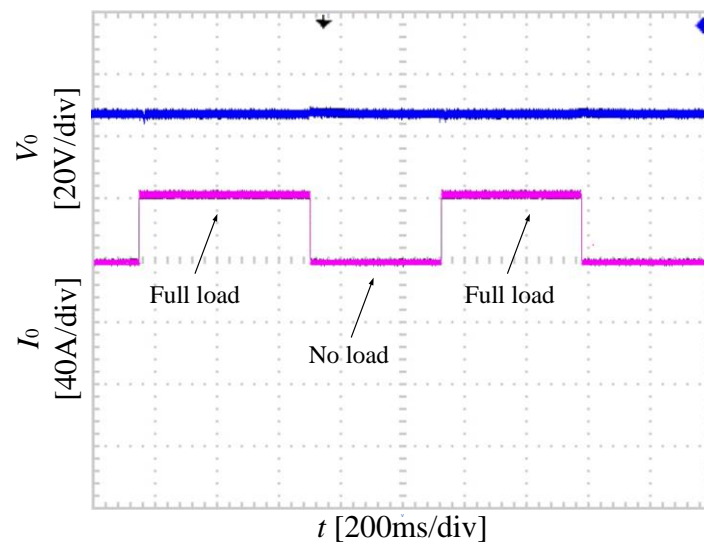


Figure 35. Load change experimental waveform.

Figure 36 shows the efficiency curves of the experimental data for different input voltages at a rated full load for different control methods, including compound control and conventional FM control. The input voltages between 300 V and 600 V all reach over 90% efficiency under compound control. A maximum efficiency of 95.3% is reached at the control-switching point, which is a 1.3% increase in maximum efficiency compared to conventional FM control. The converter achieves efficient conversion over the full voltage range.

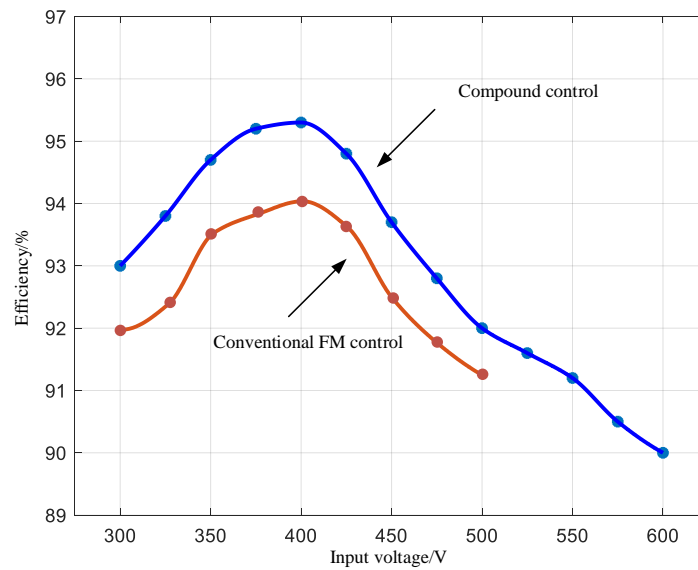


Figure 36. Efficiency curve at rated full load.

Figure 37 shows the comparison of the component losses between the compound control and conventional FM control under full load conditions. It can be seen that the total losses of the converter operating at a full load under compound control amount to 94 W at the mode-switching point. The total losses in the conventional FM control equate to 120 W. The compound control reduces losses by 26 W compared to the conventional FM control.

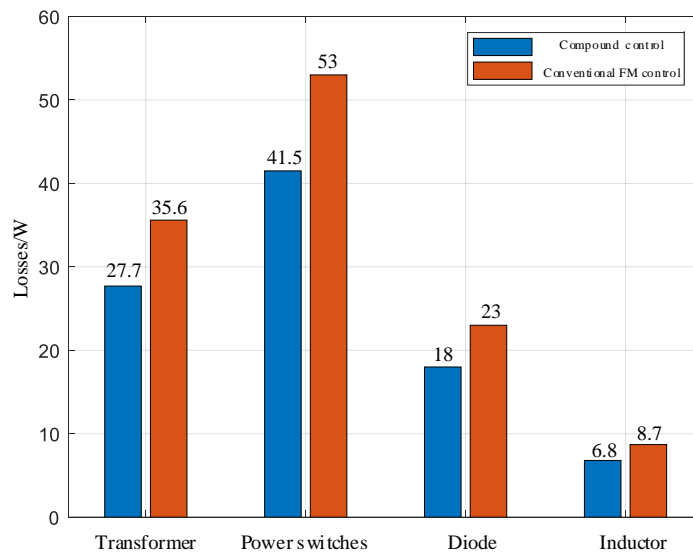


Figure 37. Loss analysis comparison graph.

7. Conclusions

In this study, through the circuit topology’s establishment, the composite control strategy’s design, and the analysis of the results, a wide input voltage on-board DC/DC converter based on an LLC resonant converter was designed. The main findings are summarized as follows.

The system characteristics were analyzed according to the design requirements of the on-board DC/DC converter, which uses a full-bridge LLC resonant converter and achieves zero-voltage activation of the switching transistors through resonant elements.

In terms of the control strategy, to adapt to wide input voltage operating conditions, combining the advantages of a frequency modulation control strategy and phase shift

control strategy, a composite control strategy has been proposed. Its control principle was then analyzed. Afterwards, the selection of the switching point of the control mode was discussed, and the switching point voltage was finally derived.

Simulation software was used to build the LLC resonant converter model. The obtained results verify the effectiveness of the composite control strategy of the LLC resonant converter. An experimental platform was then built. The LLC resonant converter achieved stable operation with an input voltage in the range of 300 V–600 V and an output voltage of 48 V. Soft switching was achieved in both the FM and phase shift control modes, and the experimental results verified the feasibility of the design.

Author Contributions: Conceptualization, K.Z.; supervision, X.W.; writing—review and editing, Y.L. All authors have read and agreed to the published version of the manuscript.

Funding: This work was supported by the Open Fund Project of State Key Laboratory of Automotive Safety and Energy (No. KFY2222).

Conflicts of Interest: The authors declare no conflict of interest.

References

1. Hao, X.; Yuan, Y.; Wang, H.; Ouyang, M. Plug-in hybrid electric vehicle utility factor in China cities: Influencing factors, empirical research, and energy and environmental application. *eTransportation* **2021**, *10*, 100138. [[CrossRef](#)]
2. Gou, C.; Zhu, K.; Chen, C.; Xiao, X. Characteristics and effect laws of the large-scale electric Vehicle's charging load. *eTransportation* **2020**, *3*, 100049.
3. Gan, L. 48V Light Hybrid Vehicle General Arrangement Design and Control Strategy Research. Master's Thesis, Hefei University of Technology, Hefei, China, 2020.
4. Shi, B.; Yang, F.; Hu, C.; Ouyang, M. Modelling and improvement of oscillation problem in a double-sided LCC compensation network for electric vehicle wireless power transfer. *eTransportation* **2021**, *8*, 100108. [[CrossRef](#)]
5. Yi, K.; Moon, G. Novel Two-Phase Interleaved LLC Series-Resonant Converter Using a Phase of the Resonant Capacitor. *IEEE Trans. Ind. Electron.* **2009**, *56*, 1815–1819.
6. Chen, G.; Zhou, Y.; Ding, Z.; Zeng, J. A Three-Leg-Based Full-Bridge Converter with Wide Input Voltage Range. *IEEE Trans. Ind. Electron.* **2021**, *69*, 5690–5699. [[CrossRef](#)]
7. Yang, D.; Duan, B.; Ding, W. A Wide Input Voltage Range LLC Resonant Converter with Auxiliary Bidirectional Switching Unit. *Trans. CES* **2020**, *35*, 775–785.
8. Lee, S.; Lee, B.; Kwon, D. Two-Mode Low-Voltage DC/DC Converter with High and Wide Input voltage Range. *IEEE Trans. Ind. Electron.* **2020**, *68*, 12088–12099. [[CrossRef](#)]
9. Gui, X. Study of Digital Wide Input Range LLC Converters. Master's Thesis, Shaanxi University of Science and Technology, Xian, China, 2020.
10. Sun, W.; Xing, Y.; Wu, H. Modified high-efficiency LLC converters with two split resonant branches for wide input-voltage range applications. *IEEE Trans. Power Electron.* **2017**, *33*, 7867–7879. [[CrossRef](#)]
11. Liu, R.; Wang, Y.; Han, F. Two-Mode Switching Soft-Switching Resonant DC Converter for Wide Input Voltage Range. *Trans. CES* **2020**, *35*, 4739–4749.
12. Deng, J.; Li, S.; Hu, S. Design Methodology of LLC Resonant Converters for Electric Vehicle Battery Chargers. *IEEE Trans. Veh. Technol.* **2014**, *63*, 1581–1592. [[CrossRef](#)]
13. Musavi, F.; Craciun, M.; Gautam, D. An LLC Resonant DC-DC Converter for Wide Output Voltage Range Battery Charging Applications. *IEEE Trans. Power Electron.* **2013**, *28*, 5437–5445. [[CrossRef](#)]
14. Wu, H.; Li, Y.; Xing, Y. LLC Resonant Converter with Semi-Active Variable-Structure Rectifier (SA-VSR) for Wide Output Voltage Range Application. *IEEE Trans. Power Electron.* **2015**, *31*, 3389–3394. [[CrossRef](#)]
15. Shakib, S.; Mekhilef, S. A Frequency Adaptive Phase Shift Modulation Control Based LLC Series Resonant Converter for Wide Input Voltage Applications. *IEEE Trans. Power Electron.* **2016**, *32*, 8360–8370. [[CrossRef](#)]
16. Xiong, J.; Yang, D.; Huang, G. Ultra-Wide Input Range Three-Level LLC Converter and Control Strategy. *Power Electron.* **2021**, *55*, 104–107.
17. Wei, Y.; Luo, Q.; Mantooth, H. Hybrid Control Strategy for LLC Converter With Reduced Switching Frequency Range and Circulating Current for Hold-Up Time Operation. *IEEE Trans. Power Electron.* **2021**, *36*, 8600–8606. [[CrossRef](#)]
18. Wang, M.; Pan, S.; Zha, X. Hybrid Control Strategy for An Integrated DAB-LLC-DCX DC-DC Converter to Achieve Full-Power-Range Zero-Voltage Switching. *IEEE Trans. Power Electron.* **2021**, *36*, 14383–14397. [[CrossRef](#)]
19. Inam, W.; Afridi, K.; Perreault, D. Variable Frequency Multiplier Technique for High-Efficiency Conversion Over a Wide Operating Range. *IEEE J. Emerg. Sel. Top. Power* **2015**, *4*, 335–343. [[CrossRef](#)]
20. Sun, X.; Qiu, J.; Li, X. An Integrated Buck-Boost LLC Cascade Converter with Wide Input Voltage Range. *Proc. CSEE* **2016**, *36*, 1667–1673.

21. Sun, X.; Li, X.; Shen, Y.; Wang, B. Dual-Bridge LLC Resonant Converter with Fixed-Frequency PWM Control for Wide Input Applications. *IEEE Trans. Power Electron.* **2017**, *32*, 69–80. [[CrossRef](#)]
22. Khan, S.; Sha, D.; Jia, X.; Wang, S. Resonant LLC DC-DC Converter Employing Fixed Switching Frequency Based on Dual-Transformer With Wide Input-Voltage Range. *IEEE Trans. Power Electron.* **2021**, *36*, 607–616. [[CrossRef](#)]
23. Zhou, K.; Gu, F.; Yang, J. Research on Dual Output Port LLC Circuit and Its Control Technology. *Electr. Mach. Control* **2021**, *25*, 17–26.
24. Li, J.; Ruan, X. Composite control strategy for Full-Bridge LLC Resonant Converters. *Trans. CES* **2014**, *28*, 72–79.
25. Ausnain, N.; Sahin, S.; Saffet, A. Impact of electric vehicle aggregator with communication time delay on stability regions and stability delay margins in load frequency control system. *J. Mod. Power Syst. Clean Energy* **2021**, *3*, 595–601.
26. Sun, X.; Shen, Y.; Zhu, Y. A Boost Type Wide Voltage Range Input LLC Resonant Converter. *Proc. CSEE* **2015**, *34*, 3895–3903.
27. Yin, Q.; Wang, Z.; Zhou, L. Light-Load Time Domain Model of A Full-Bridge LLC Resonant Converter. *Power Electron.* **2019**, *53*, 4–7.
28. Liu, T.; Yang, X.; Ge, S.; Leng, Y.; Wang, C. Ultrafast charging of energy-dense lithium-ion batteries for urban air mobility. *eTransportation* **2021**, *7*, 100103. [[CrossRef](#)]
29. Fachrizal, R.; Shepero, M.; Meer, D.; Munkhammar, J. Smart charging of electric vehicles considering photovoltaic power production and electricity consumption: A review. *eTransportation* **2020**, *4*, 100056. [[CrossRef](#)]